A WIDE DYNAMIC RANGE SWITCHING CURRENT REGULATOR FOR COST EFFICIENT MAGNETIC ATTITUDE CONTROL OF NANOSATELLITES

By

Carl Haken

Senior Thesis in Electrical Engineering

University of Illinois at Urbana-Champaign

Advisor: Professor Gary R. Swenson

May 2016

Abstract

CubeSats are an increasingly popular platform for performing scientific research in space at a low cost. Traditional propulsive or reaction wheel based attitude control systems are complex, expensive, and require a large percentage of the nanosatellite's volume. In this project, a low cost, low volume magnetic attitude control actuator is presented for CubeSats. The overall design is explored, with a focus on the switch mode wide dynamic range current regulator, which is built using discrete components. Results are presented, including efficiencies in excess of 95%, current set point error of less than 1%, fast and damped step responses, and output voltage ripple below 50 mV peak-to-peak. The cost and volume of the controller compare favorably to available commercial magnetic attitude controllers.

Subject Keywords: CubeSats; Attitude Control; Magnetorquer; Current Regulator; Analog Feedback

Acknowledgments

This work is the culmination of my undergraduate efforts in the areas of power electronics and practical satellite building. Of the projects I have worked on, this one has taken the most time and taught me the most about engineering. I would like to acknowledge the individuals who have made this project possible for me: aerospace postdoc Alex Ghosh, aerospace graduate students Erik Kroeker and Pat Haddox, former ECE student Zipeng Wang, the staff of the ECE electronics service shop, my summer internship mentor Nick Spera, and of course my advisor Professor Gary Swenson. I would also like to thank the organizers and sponsors of ECE395 (ADSL) and the Grainger CEME UR&L Award for the support and resources they have provided. Their help and support have been invaluable for making this project a success.

Contents

1. Introduction

1.1 CubeSats

Nanosatellites are an increasingly popular platform for performing scientific research in space at a relatively low cost. CubeSats are a common type of nanosatellite characterized primarily by their standardized size and shape. CubeSats are described in terms of "Units" or "U", where one U is a 10x10x10 cm volume. CubeSat volumes are generally integer multiples of 1U, which allows launch providers to flexibly launch either a few large CubeSats or many small ones with the same support structure. The University of Illinois at Urbana-Champaign has an active CubeSat project headed by Aerospace Engineering professor Victoria Coverstone and Electrical Engineering professor Gary Swenson. The primary goal of the project is to develop the IlliniSat-2 CubeSat bus, which consists of all systems necessary for operating a satellite except the science payloads, and to launch science missions using this bus. The 6U LAICE and 3U CubeSail missions will be the first two missions to fly using the IlliniSat-2 bus in late 2016, both with NSF-funded scientific payloads. This thesis describes the IlliniSat-2's torque coils, which are the attitude control actuators that I have been designing over the past two years.

1.2 Magnetic Attitude Control

A satellite's attitude refers to the direction in which it is pointing and the speed and direction in which it is spinning. Nearly all satellites require some form of attitude control in order to point their instruments in the right direction. Large satellites tend to use chemical propellants or electrically actuated reaction wheels. Such systems are bulky and expensive, and are not without inherent problems. Chemical propellants can be exhausted and are difficult to handle on the ground. Reaction wheels have a finite limit on their rotational speed in a given direction, so they cannot correct for small recurring torques indefinitely. A third option in low earth orbit is magnetic attitude control. The satellite generates a magnetic field that attempts to align itself with the earth's magnetic field, producing a torque on the satellite. Magnetic attitude control systems tend to be weak compared to the other methods, but they are smaller, easier to handle, less expensive. Large satellites sometimes use magnetic attitude control to dump momentum out of their more powerful reaction wheel systems. Small satellites often use magnetic attitude control exclusively. Magnetic attitude control systems are called magnetorquers. There are two kinds of magnetorquers: torque rods and torque coils. Torque rods run current through a wire wrapped around a magnetic core, and they rely on the magnetization of the core to efficiently produce large magnetic moments. The area of any individual loop of wire tends to be small. Torque coils run current through a flat coil with no core, and they rely on the relatively large area of the individual loops to produce large magnetic moments. My design is a torque coil design. Throughout this paper, unless otherwise specified, the term "torque coil" refers to the specific piece of hardware that I designed in this project. The torque coils are part of the IlliniSat-2's Attitude Determination and Control System (ADCS), which also includes magnetometers and sun sensors for attitude determination, and the central processor that runs the control algorithm.

1.3 How This Project Fits In

The physics functionality of a magnetorquer can be derived from two simple magnetics equations. Equation (1) is the magnetic moment $\vec{\mu}$ for a flat, layered coil with a current flowing through it. In this case, A_{coil} is the sum of the area of each loop on a given layer, and N_{layers} is the total number of layers in the coil. Equation (2) is the torque that acts on a magnetic moment in the presence of an ambient magnetic field.

$$\vec{\mu} = N_{layers} i_{coil} A_{coil} \tag{1}$$

$$\vec{\tau} = \vec{\mu} \times \vec{B}_{ambient} \tag{2}$$

The number of layers and the area of the coil is constant for a given torque coil. Therefore, the magnetic moment relates linearly to the current in the coil. The ambient magnetic field changes throughout the satellite's orbit. It is up to the central ADCS processor to measure the ambient field and determine the desired torque and magnetic moment. The central processor then commands the torque coils to generate currents that will produce the desired moment and torque. The bulk of the work in this project is designing a regulator that is capable of accepting a commanded current level, and producing that current in the physical coil in an efficient and expedient manner. The location of this work within the attitude determination and control system is graphically depicted in Figure 1.

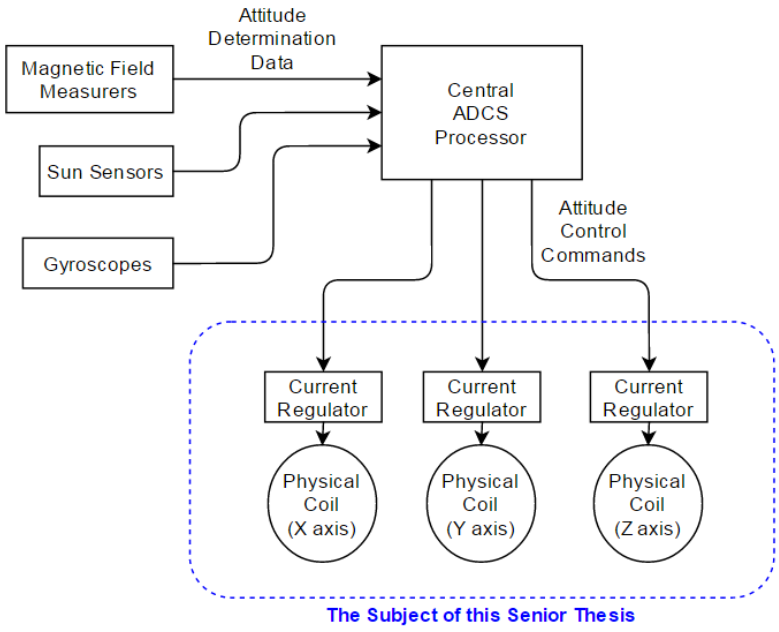

Figure 1: The attitude determination and control system of our satellite.

1.4 Nomenclature

ADCS	attitude determination and control system
ESR	equivalent series resistance
i2c	inter-integrated circuit, a standard 2-wire communications protocol
Magnetorquer	magnetic attitude control hardware
PCB	printed circuit board
PWM	pulse width modulation
RS-485	half-duplex differential communications protocol
Torque Coil	One type of Magnetorquer – a flat coil with no magnetic core. In this work, “Torque Coil” generally refers the specific torque coil that I designed.

2. Background & Literature Review

2.1 Commercially Available Solutions

There are commercially available magnetic attitude control systems for CubeSats, which we examined during the initial planning phase of this project. At the time of this writing, The CubeSatShop sells a complete 3-axis magnetorquer system for €8000, with external dimensions of 96 x 90 x 17 mm.[1] ClydeSpace sells a 1-axis magnetorquer for $1425, which is 100 x 100 x 4.3 mm and includes only the coil, not the current regulator that controls the coil.[2] Additionally, these systems have their own pre-defined connectors, voltage requirements, and communication specs that impose design constraints on the rest of our satellite. The UIUC CubeSat team estimated that we could build a similar system in a smaller volume with a substantially lower manufacturing cost based on the cost of a typical PCB, components, and professional assembly. We mitigated the development costs using economically advantageous undergraduate labor. We believed that we could achieve a smaller volume partially because of our ability to custom design the magnetorquer around the existing satellite hardware. The majority of publications relating to CubeSat attitude control are about the control algorithms and reference frame issues as opposed to the actuators. There is comparatively little published work on the hardware design of a magnetorquer system, especially on the level of circuit diagrams, partially because a good hardware design is immediately marketable.

We chose the torque coil design over the torque rod design for two reasons. Firstly, torque coils fit better into the existing satellite architecture. Secondly, the lingering magnetization of magnetic cores poses problems. The satellite depends heavily on magnetometers to measure the earth's magnetic field in order to determine the satellite's attitude. Any permanent magnets on board the satellite would compromise the accuracy of the magnetometers. The magnetic cores could be demagnetized using a degaussing sequence, but this process consumes valuable time and power, and is not guaranteed to eliminate the static field entirely. For these reasons, we decided to use torque coils, and we decided against attempting to place a small core in the center of each coil.

[1] www.cubesatshop.com/index.php?page=shop.product_details&category_id=7&product_id=102
[2] www.clyde-space.com/cubesat_shop/adcs/215_z-axis-magnetorquer

3. Requirements and Design Goals

I started this project with a detailed consideration of the requirements and design goals. The requirements are physical restrictions imposed by the existing satellite hardware, and the design goals are conceptual guides for making design decisions. The three design goals I chose were full functionality, minimizing torque error, and minimizing quiescent power draw.

3.1 Design Goals

The first design goal is to produce fully functional hardware by the end of this project. Full functionality is the most important because of the nature of this project. We have several actual satellites to launch with actual science payloads, and therefore my final product must really work. It is not acceptable to leave significant problems in a future work section.

The second design goal is minimizing torque error. Torque error is the difference between the torque that the ADCS is attempting to produce, and the torque that the satellite actually experiences. Torque error does not lead to permanent errors in satellite orientation, because the ADCS will eventually measure and correct for accumulated errors. However, consistent sources of torque error will require the satellite to spend more time and power on attitude control, which reduces time and power available for the mission's scientific objectives. Therefore, a good torque coil design will minimize torque error where possible.

The last design goal is minimizing quiescent power consumption. Our CubeSats generally have limited continuous power budgets of approximately 6 W, and an individual IlliniSat-2 CubeSat will have six torque coils so that every axis has a primary coil and a backup. Therefore, it is important for the torque coil to have low quiescent power consumption.

3.2 Requirements and Desired Properties

In order for the attitude control system to produce a torque in the desired direction, the torque coils as a whole must be able to produce magnetic moments in any arbitrary direction. With one active coil per Euclidian axis, the individual coils must produce small magnetic moments as well as large ones, and they must be able to produce a magnetic moment in either direction. Electrically speaking, this means that the current flowing in the coil must be adjustable based on software commands, and must be able to flow clockwise or counterclockwise through the coil. It follows that an individual torque coil driver must accurately generate a wide range of currents with high accuracy in order for the attitude control system to produce arbitrary magnetic moments.

There are numerous physical requirements imposed on the torque coil by the existing satellite architecture. Table 1 summarizes these requirements, which are independent of the functionality of the torque coil. The area requirement is more nuanced than described in the table. Small cutouts are required in all four corners in order to accommodate existing unrelated screw holes, and all components must be confined to one end of the board. The torque coil's exact dimensions and component locations were checked repetitively against the 3D CAD model of the satellite to ensure that no mechanical interferences would occur. In addition to these requirements, the torque coil must strive to satisfy

numerous competing desired properties. Table 2 summarizes the desired properties and the reasons behind them.

Table 1: Requirements imposed by existing satellite architecture.

#	Requirement	Value	Reason
1	Area	78.2 by 90.0 mm PCB	Available physical space on the satellite.
2	Microcontroller	PIC18F24K22	Already in use elsewhere on satellite.
3	Communication protocol	RS-485	Already in use elsewhere on satellite.
4	Operating temperature	-40 to +60 C	Expected satellite temperature range.
5	Input voltage range	5.5 to 8.5 V	Voltage range of satellite's battery bus.

Table 2: Desired properties of the torque coil.

#	Desired Property	Reason
1	High magnetic moment	Stronger torque
2	High magnetic efficiency (moment per unit current in coil)	Less power consumption
3	Wide range of outputs: 0-100% in 1% increments	Reduce torque error
4	Accurately controlled output: Current is with 1% of commanded value	Reduce torque error
5	Bidirectional current: one coil produces a field in either direction	Allows 1 coil per axis
6	High electrical efficiency (power into coil per unit input power)	Less power consumption
7	Low output voltage ripple (<50 mV pk-pk)	Reduce radiated EMI
8	Fast response time (<10 ms overall, <5 ms for regulator)	Reduce torque error

Properties 1 and 2 are directly in conflict when designing the physical coil. For instance, given a two layer PCB, putting the layers in parallel reduces the coil resistance, allowing for a higher current and a higher peak magnetic moment. However, putting them in series produces magnetic moment more efficiently per unit current, but the significantly higher resistance substantially reduces the peak current and therefore the peak magnetic moment. Properties 7 and 8 are also in direct conflict, as is discussed extensively in section 4.4 Bandwidth and Output Ripple.

4. Design

4.1 Block Diagram

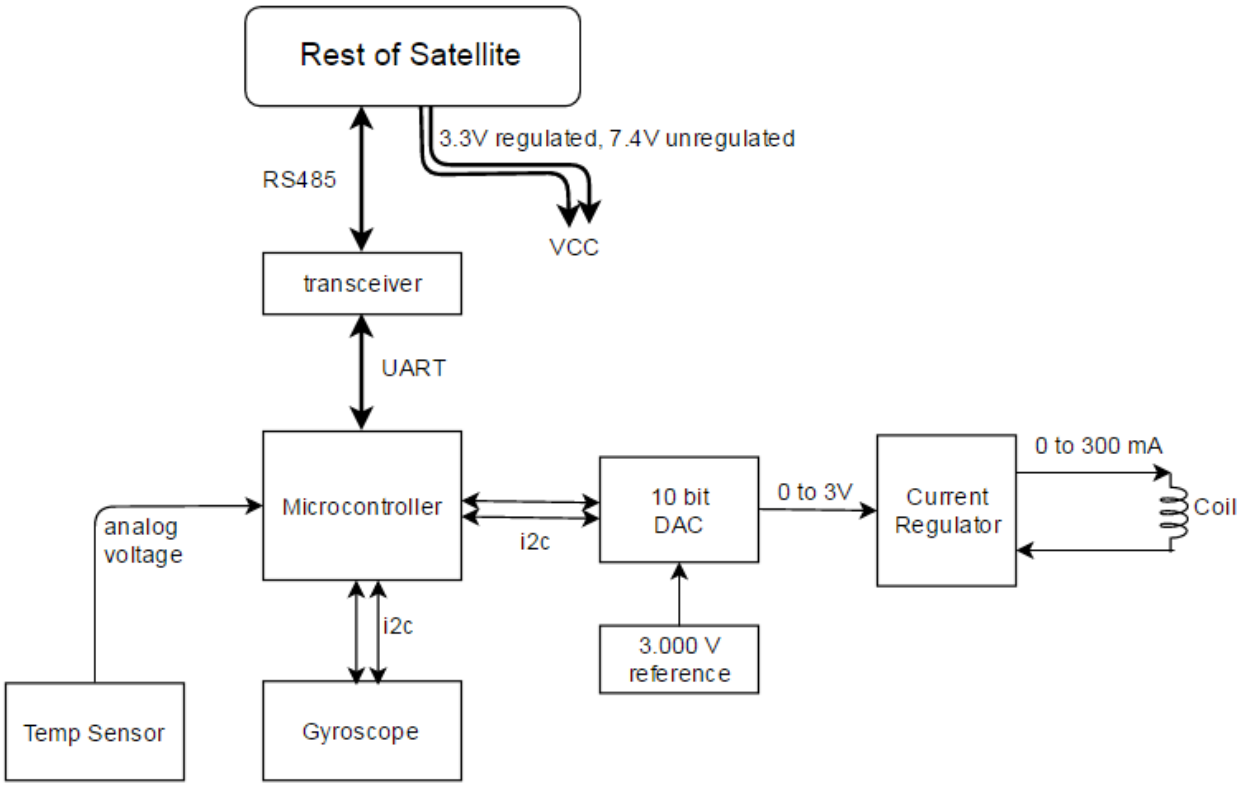

Figure 2: Torque coil block diagram

Figure 2: Torque coil block diagram shows the block diagram for the torque coil PCB. The torque coil receives a regulated 3.3 V rail and an unregulated nominally 7.4 V rail from the satellite's power board, as well as an RS485 differential signaling pair. The microcontroller receives commands and sends replies using a transceiver. The microcontroller has an attached temperature sensor and gyroscope. These sensors are part of the satellite's overall sensing system, and they are on the torque coil because it is useful to have them there from a satellite design perspective, but they have nothing to do with producing a magnetic moment. In order to produce a magnetic moment, the microcontroller sends a command to the DAC, which sends a corresponding analog voltage to the current regulator. The current regulator then drives a current through the coil proportional to the reference voltage. I chose an external DAC because the microcontroller's internal one is only 5 bits, which is not sufficient resolution.

4.2 Regulator Architecture

When designing the torque coil current regulator, my first instinct was to use an off-the-shelf variable voltage regulator to drive the coil. This approach assumes that the coil has a constant resistance, which is not a safe assumption. The coil is made of copper, so its resistance changes significantly with temperature. The satellite's temperature could potentially vary by more than 50 C during a single orbit. In addition, if one side of the satellite is in sun and the other is shaded, the torque

coils on the sunny side will be noticeably warmer. I could measure the temperature and attempt to guess the resistance, but the act of operating the coil directly warms the copper through ohmic heating, so any temperature measurement scheme would be prone to error. With these requirements in mind, I decided to build a current regulator instead. I had significant difficulties finding off-the-shelf regulator chips that claimed to be able to regulate to a wide enough range of voltages or currents. Most small package adjustable voltage regulators simply will not output voltages below 0.6 or 0.8 V. Among other things, I tried two variable output voltage regulators, and one constant current battery charger chip, but none of them worked. Even the circuits that worked in simulation failed in practice. The variable voltage regulators could not cover the required range of outputs when implemented in hardware, and the battery charger became partially unstable with a large unexplained 3-6 kHz output ripple when driven to output voltages above 5 V. Therefore, I instead decided to design my own current regulator using discrete components.

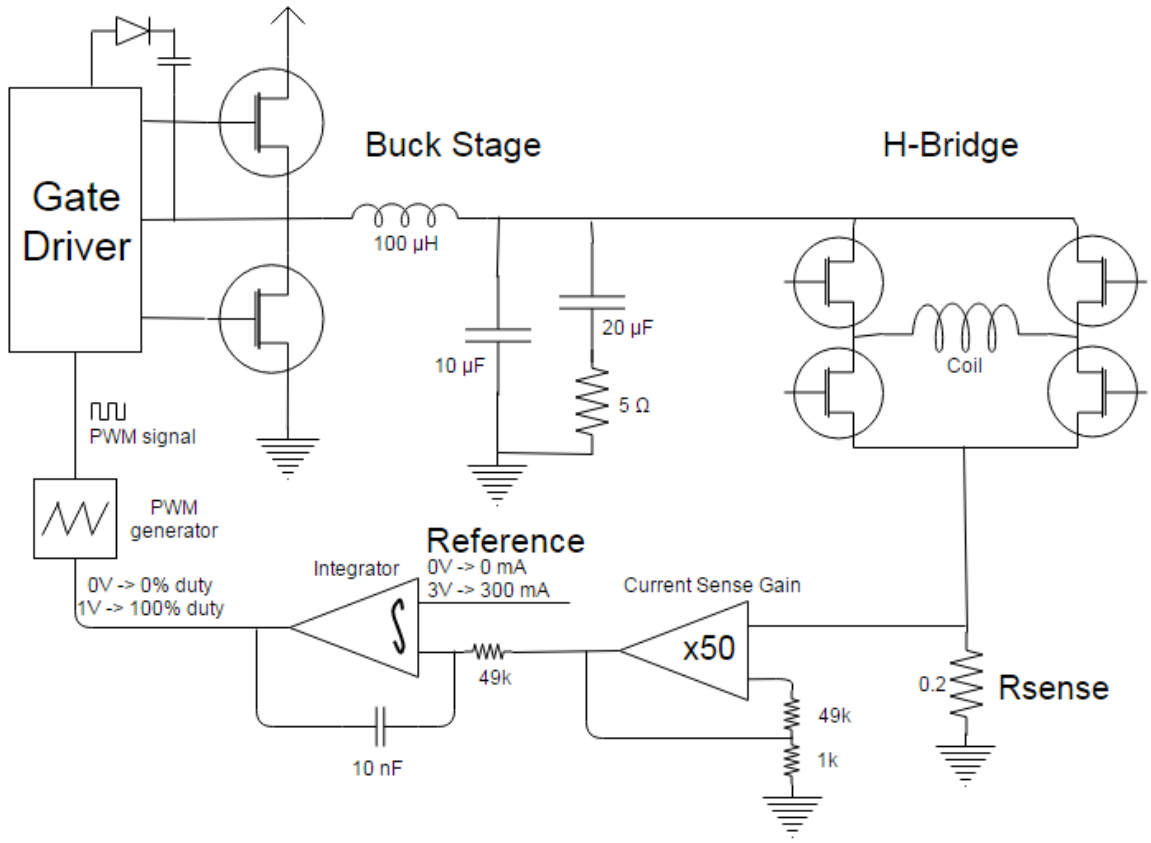

Figure 3: Current regulator schematic.

Figure 3 shows a schematic diagram of the current regulator I designed. The next few sections will discuss the individual components in detail, and will refer back to this figure. I based most of the passive component values on my simulations. The 100 µH inductor is the exception, I made it as large valued as possible in order to minimize the ripple current. High ripple current is a large source of loss in

low duty-cycle buck converters, and I saw efficiency improvements of over 15% under some operating conditions when I increased the inductor value from 22 µH to 100 µH.

4.3 Control Scheme

4.3.1 Analog vs Digital

I chose to design the regulator with analog control rather than digital, despite having a microcontroller already in the design. The torque coil uses a PIC18F24K22 microcontroller for the sake of simplicity and consistency, because several other peripheral systems such as the magnetometers and flex cables already use that microcontroller. With an 8 MHz oscillator, the PIC18F24K22 is capable of only about 5.5 bits of PWM duty cycle resolution at 100 kHz. This low resolution is already too low to allow for 100 discrete steps between off and full power, as is desired to minimize torque error. A 32 MHz oscillator would allow for 8 bits of precision at 100 kHz, which would be sufficient; however, it would also increase the microcontroller's quiescent current draw to about 10 mA, which is an undesirably large amount compared to 2.5 mA at 8 MHz. I decided that I would be able to achieve both low quiescent current consumption and high resolution at 100 kHz by using an analog control loop. Table 3 in chapter 5. Results lists the current draw of the components in the final design, and the results validate my decision. A 7.5 mA increase in microcontroller current draw would more than double the quiescent power consumption of the coil.

4.3.2 Feedback Component Selection

I used the LT1783 op amp for both the current sensing gain and the analog integrator, as seen at the bottom of Figure 3. I chose this op amp for its low power consumption, low input offset voltage, shut down pin, and general fulfillment of my circuit's requirements. I chose a sense resistor of 0.2 Ω and a gain of 50 so that a 300 mA current would correspond to a 3.0 V voltage. A smaller sense resistor would improve efficiency, but the larger the gain, the more susceptible the circuit is to noise. I used two LTSpice simulations to size the integrator's resistor and capacitor, as discussed in a later section. The RC time constant of the integrator relates directly to the bandwidth of the regulator. Selecting the correct bandwidth is a complex problem, as discussed in the next section.

4.4 Bandwidth and Output Ripple

4.4.1 Introduction to the Problem

The resonant frequency of a buck converter's inductor and output capacitor dominates the process of designing a control loop for a buck converter. At the resonant frequency, there exists a double pole that causes a sharp 180-degree drop in the phase. This results in instability if the feedback loop has a gain greater than unity at or above the resonant frequency. In addition, the undamped double pole causes a significant upward spike in the gain of the system. Figure 4 shows a Bode plot of my current regulator exhibiting this problem. Therefore, when using a simple PI controller, also called a Type I compensator in power electronics, it is necessary to make the bandwidth significantly lower than the resonant frequency. This creates a direct conflict between the goals of reducing the response time and reducing the output ripple. A larger LC filter will result in lower output ripple, but also in a lower resonant frequency and therefore a lower bandwidth. There are two common solutions to this problem,

which both revolve around allowing the bandwidth to be near the LC resonance instead of significantly below it. The first is a Type III compensator, which is essentially a double lead controller that places two zeros at a lower frequency than the LC resonance, and two poles at a higher frequency. This controller creates a temporary phase boost of up to 180 degrees around the LC resonance, allowing the system to have a bandwidth near the resonant frequency while maintaining a positive phase margin. To realize a Type III compensator, add a series resistor-capacitor pair in parallel with the resistor and capacitor of a standard integrating op amp. The Type III compensator relies on a high level of stability in the feedback network's passive components and the output filtering components. This is undesirable for several reasons. Firstly, the capacitance of large valued ceramic capacitors changes significantly with bias voltage. Secondly, the satellite will experience significant temperature swings while in orbit, which can affect the exact values of passive components. The other popular choice is current mode control, in which the peak current in the inductor is limited to some value on a cycle-by-cycle basis. This effectively turns the inductor into a current source and eliminates the output resonance. Current mode control is difficult to implement because it requires measuring the inductor current with a bandwidth higher than the switching frequency. Additionally, current mode systems suffer from subharmonic oscillation problems. I chose not to implement a current mode control system because I was not confident I could get such a system to work before the deadline. Instead of these, I developed and implemented a unique compensation strategy that works in this specific application. Figure 5 shows the updated control loop, with damping.

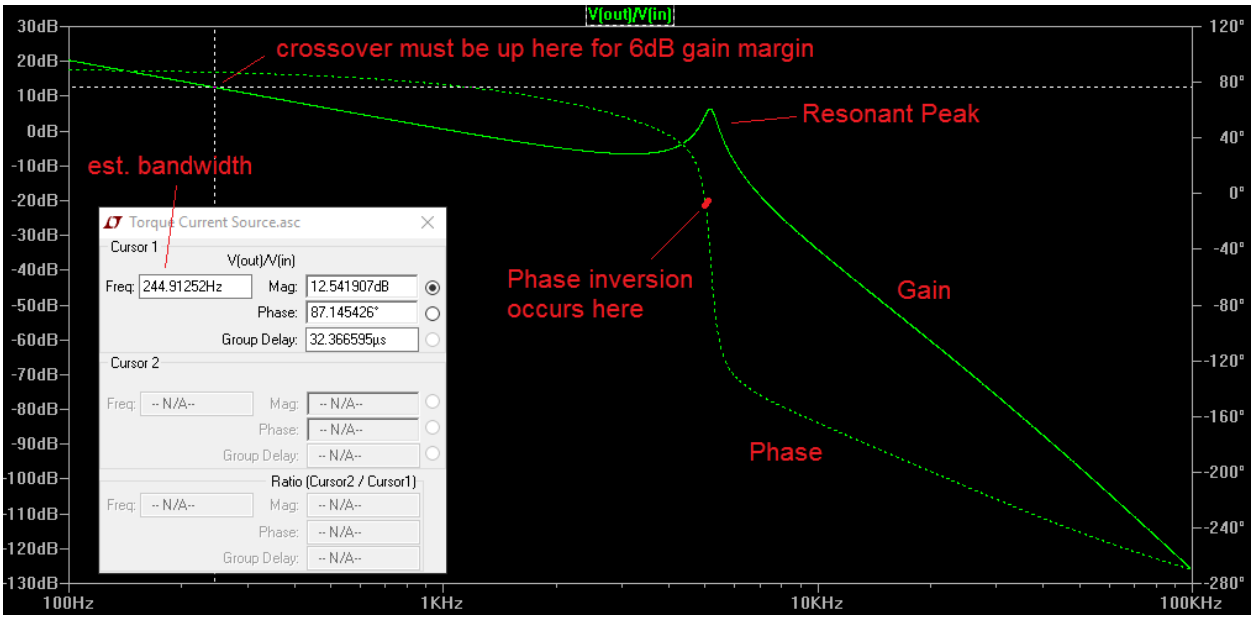

Figure 4: Bode plot for the current regulator's control loop with undamped resonant peak.

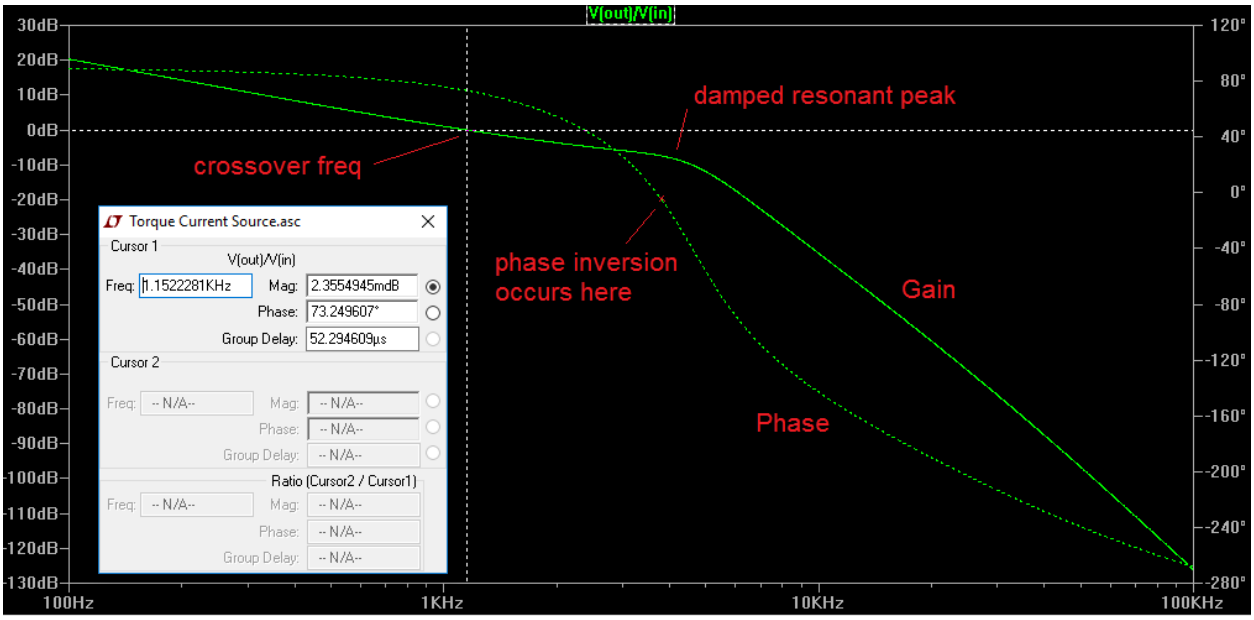

Figure 5: Bode plot for the current regulator's control loop, with damping, 1.15 kHz bandwidth, and 73-degree phase margin.

4.4.2 Damped Output Capacitor

To solve the output resonance problem, I added a series resistor-capacitor in parallel with the output capacitor, as shown in Figure 3. This damps the resonant peak in the same way that adding ESR to the main output capacitor would. With the resonant peak damped, I am free to move the crossover frequency close to the resonant peak, which enables both a fast response time and low output ripple. The bandwidth of the converter exceeds 1 kHz. To size the damping capacitor and resistor, I relied on a technique I learned for removing the resonant peaks from a generic CLC filter. The damping capacitor is approximately twice the value of the main output capacitor. To size the damping resistor, I tried values in the 0.1 to 10 Ω range and observed the resulting impedance verses frequency of the output inductor, capacitor, and damping capacitor in simulation. When the transition from capacitive to inductive slope is smoothly rounded, the resistance value is correct.

Under normal circumstances, adding ESR to the output capacitor is a bad idea because it burns a lot of power. However, adding the parallel damping resistor-capacitor is not equivalent to simply adding ESR to the main output capacitor. This is because high frequency currents can still flow through the main output capacitor without dissipating much power. Nevertheless, this setup is likely to waste power if used in a conventional power supply because any time the load changes, the damping resistor will dissipate some power. Fortunately, the torque coil is an extremely consistent load that changes only with temperature on a scale of tens of seconds or more. This means that the output voltage is essentially a DC voltage plus switching frequency ripple. At DC, the capacitors pass no current, and so their ESR is irrelevant. At the switching frequency, the damping resistor will dissipate some power. The voltage across the damping resistor, V_r, can be calculated using equation (3) using the output RMS switching frequency ripple. The power dissipation can be calculated using equation (4).

$$V_r = \left| \frac{R_{damp}}{R_{damp} + j2\pi f_{sw} C_{damp}} \right| * V_{RMS\ ripple} \quad (3)$$

$$P_{loss} = \frac{V_r^2}{R_{damp}} \quad (4)$$

Solving equations (3) and (4) for a damping resistance of 5 Ω, damping capacitance of 20 µF, switching frequency of 100 kHz, and RMS voltage ripple of 18 mV RMS, yields a damping power loss of 8.85 µW, which is negligible. The 18 mV RMS ripple corresponds to 50 mV of peak-to-peak ripple, which is the design goal for output voltage ripple.

4.5 Switches and Drivers

I originally wanted to use one Nmos and one Pmos transistor for the switching regulator. I wanted to avoid using the standard double Nmos bootstrap gate driver because that would reduce the regulator's maximum output voltage due to duty cycle limits. However, I discovered that I was unable to find a satisfactory gate driver for the Nmos/Pmos setup because no one uses Pmos transistors in power applications. The gate driver must have built-in dead time when driving the switches because implementing dead time discretely in analog requires numerous components and a lot of hardware trial and error. The gate driver must have a shut-down pin, so that the transistors are not turned on and off while the PWM generator is starting up or while the H-bridge is reversing direction. Small off-the-shelf gate drivers also are typically set up for driving Nmos transistors exclusively, which means that when they shut down, they default to pulling their outputs low. This means that the Pmos transistor will turn fully on if the converter shuts down. In addition, it is difficult to find good gate drivers with fractional milliamp quiescent currents, and low quiescent current is a major goal of this design. Eventually, I settled for a low quiescent current bootstrap driver with built-in dead time, and two Nmos transistors. The driver I chose is the TPS2836, and the Nmos transistor part number is DMN3404L.

4.6 Simulation

4.6.1 Transient Model

I used two LTSpice simulations to verify the design of the current regulator. The first simulation, shown in Figure 6: LTSpice circuit for transient analysis, is for analyzing the converter's transient response and output voltage ripple. The circuit includes models of the actual PWM generator and feedback op amps, which come with LTSpice. I replaced the gate drivers with ideal voltage controlled voltage sources. The coil of traces is modeled as a 28 Ω resistance in series with a 600 µH inductance. These values are mathematical estimates, which are acceptable because the current regulator's properties are not very sensitive to the exact resistance and inductance values of the load. Figure 7 shows an example of a transient response. The coil starts out producing 100 mA, and is commanded to produce 200 mA instead after 5 ms.

4.6.2 Linearized AC Model

The second model, shown in Figure 8, is for analyzing the stability of the control loop. I extracted Bode plots for the gain and phase of the control loop directly from the simulation by inserting an AC

source in series with the control loop path, and then sweeping the AC source across a range of frequencies. In this case, the gain is the “output” voltage divided by the “input” voltage, where the “output” voltage is coming out of the control loop towards the AC source, and the “input” voltage is going back into the loop from the AC source. Unfortunately, AC sweeps do not work on circuit models that include switching elements. This is because of how LTSpice performs AC sweeps: at each frequency, it calculates a single operating point, linearizes the circuit about that operating point, and then applies the AC signal to the linearized circuit. No transient simulation occurs, which means no time passes, which means switching elements cannot switch. Therefore, I replaced the switching elements with a linearized model. I replaced the PWM generator, gate drivers, and switches in a buck converter with a single ideal gain proportional to the duty cycle. This approximation is accurate for frequencies significantly below the switching frequency. In this case, the switching frequency is 100 kHz, which is significantly above the estimated 1 kHz bandwidth.

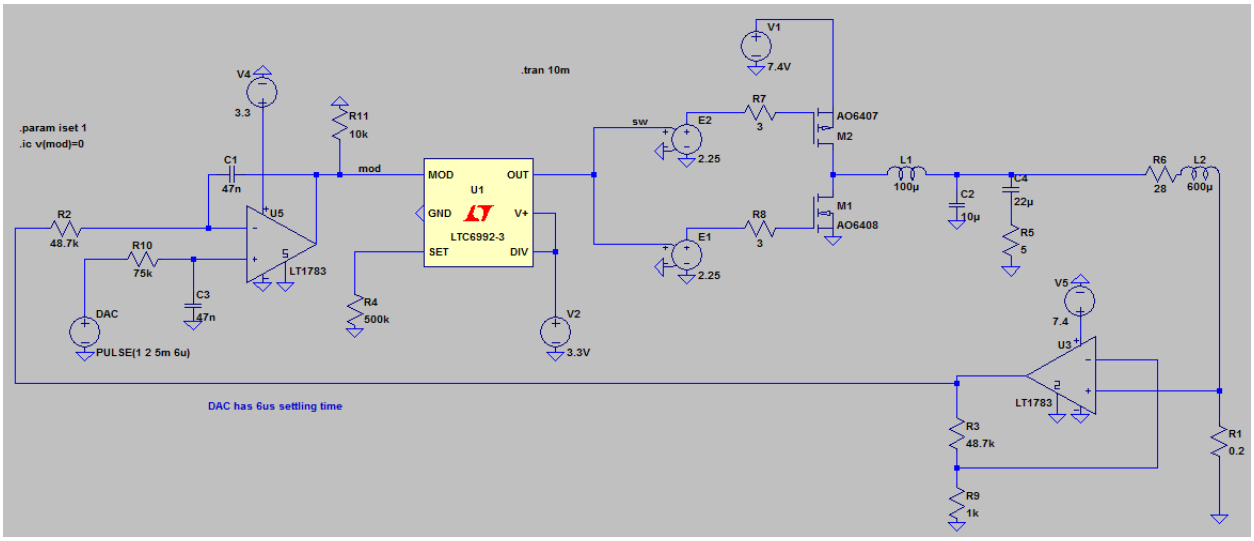

Figure 6: LTSpice circuit for transient analysis.

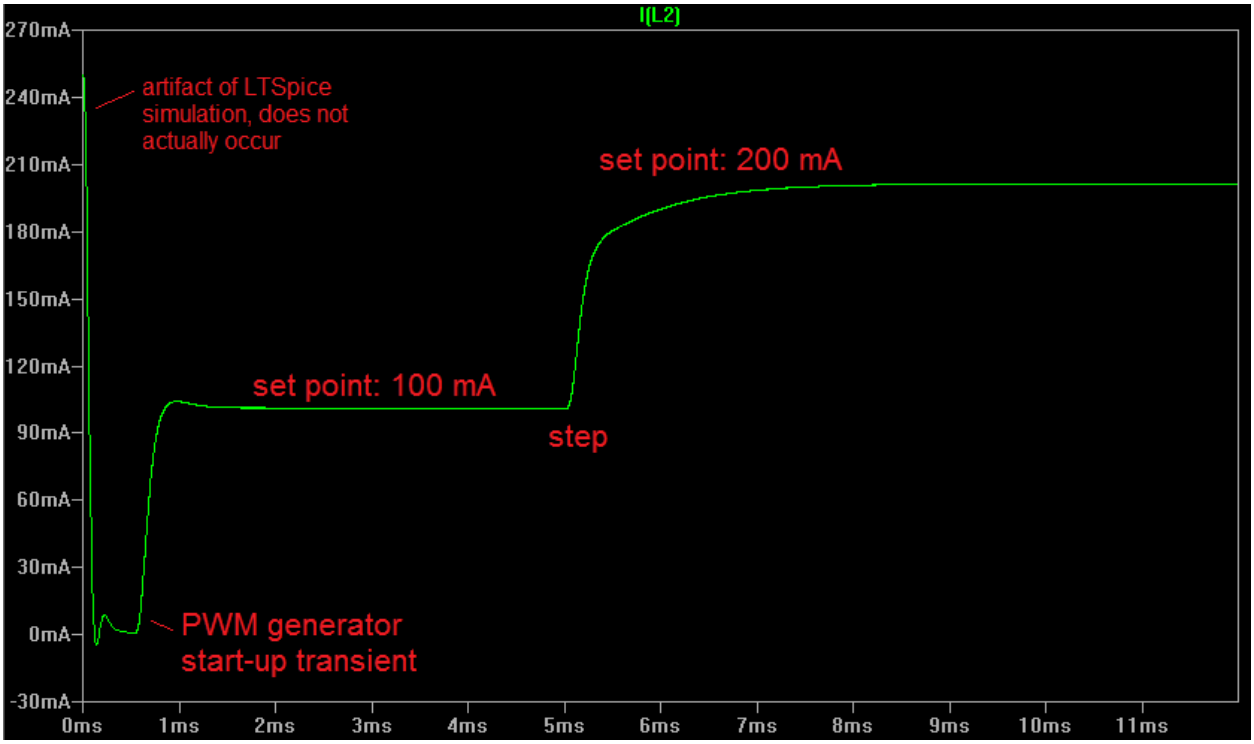

Figure 7: Transient analysis of the current regulator. A step in desired current occurs at 5 ms.

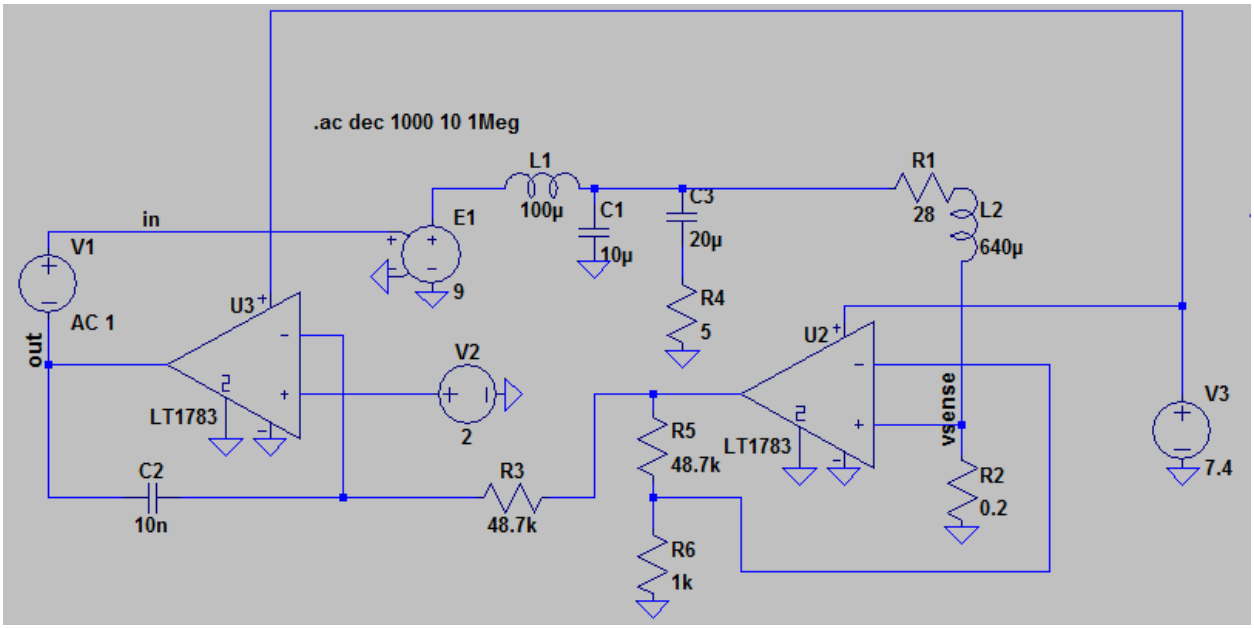

Figure 8: LTSpice circuit for feedback analysis.

4.7 PCB Layout

I performed schematic capture and PCB layout for the torque coil in EAGLE. The layout work required a significant amount of learning about practical PCB concerns because I needed to squeeze the regulator into as small a space as possible. Figure 9 shows the routing of the current regulator. The coil has 57 loops with a 22 mm diameter open area in the center. The exact number of loops is an optimized value that was determined by Aerospace Engineering graduate student Pat Haddox as the optimal trade-off between more torque and higher efficiency.

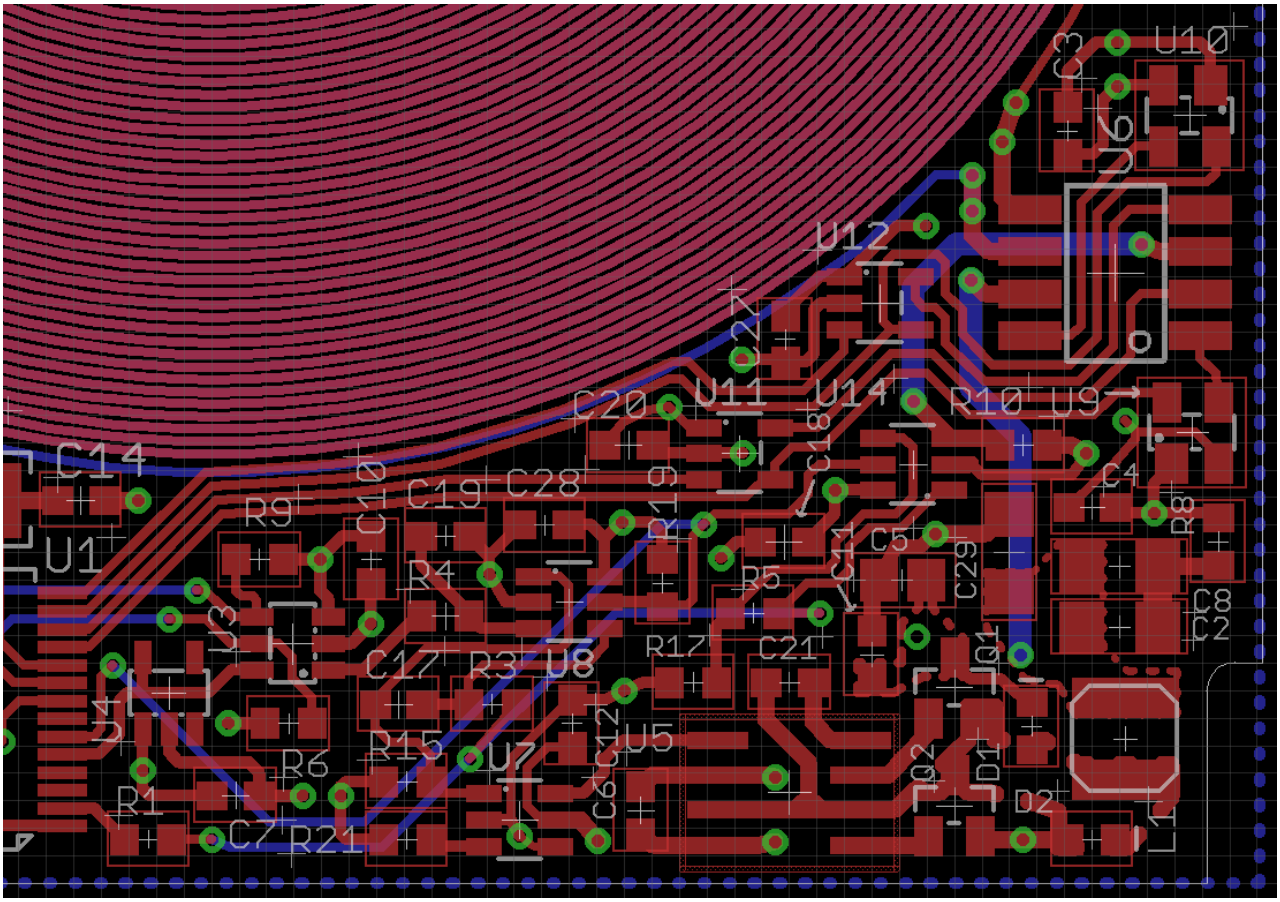

Figure 9: Part of torque coil EAGLE layout. Clockwise, from top left: Part of the coil, the H-bridge, the buck stage, the analog control loop, the 3.000V reference and DAC, and the microcontroller.

5. Results

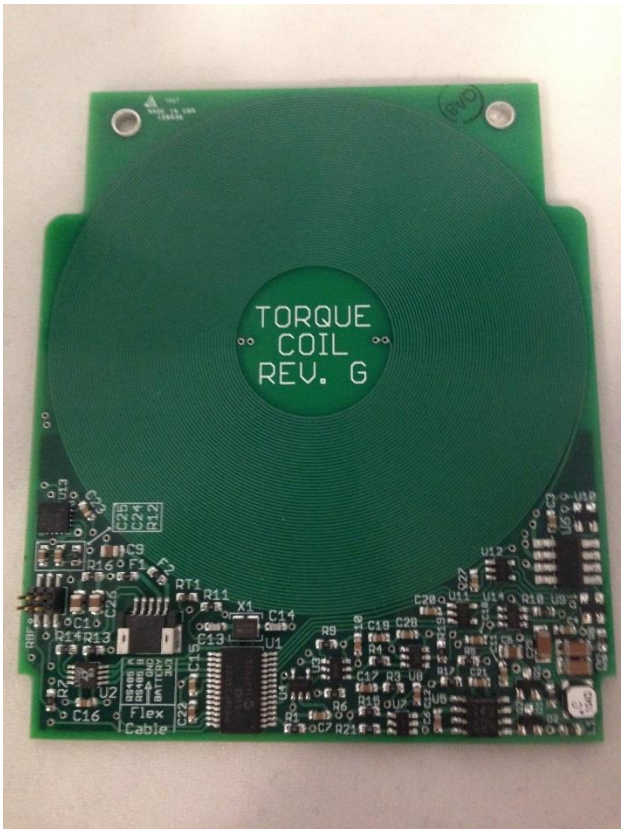

Figure 10: The final torque coil design, in hardware.

Figure 10 shows the torque coil in final hardware form. I electrically tested this coil to the extent of my abilities, and it is fully functional. This is the design that is going to space. Figure 11 shows the efficiency of the coil verses output current, at various input voltage levels. 6.0 V is the minimum battery voltage at which the coils will operate under normal conditions, and 8.5 V is the maximum voltage produced by the solar chargers. 7.4 V is the nominal battery voltage. I cannot test the current up to 300 mA, because the coil must be around -25 °C in order to be low enough resistance. We regularly expect to hit that temperature during flight, and I have tested a prototype current regulator with a resistive load to 300 mA without issues. Figure 12 shows the accuracy of the current set point, that is, the percent error between the current that the software expects, and the current that the coil produces. The inaccuracy at low currents is most likely due to offset in my current measurement technique, as these results are before calibration.

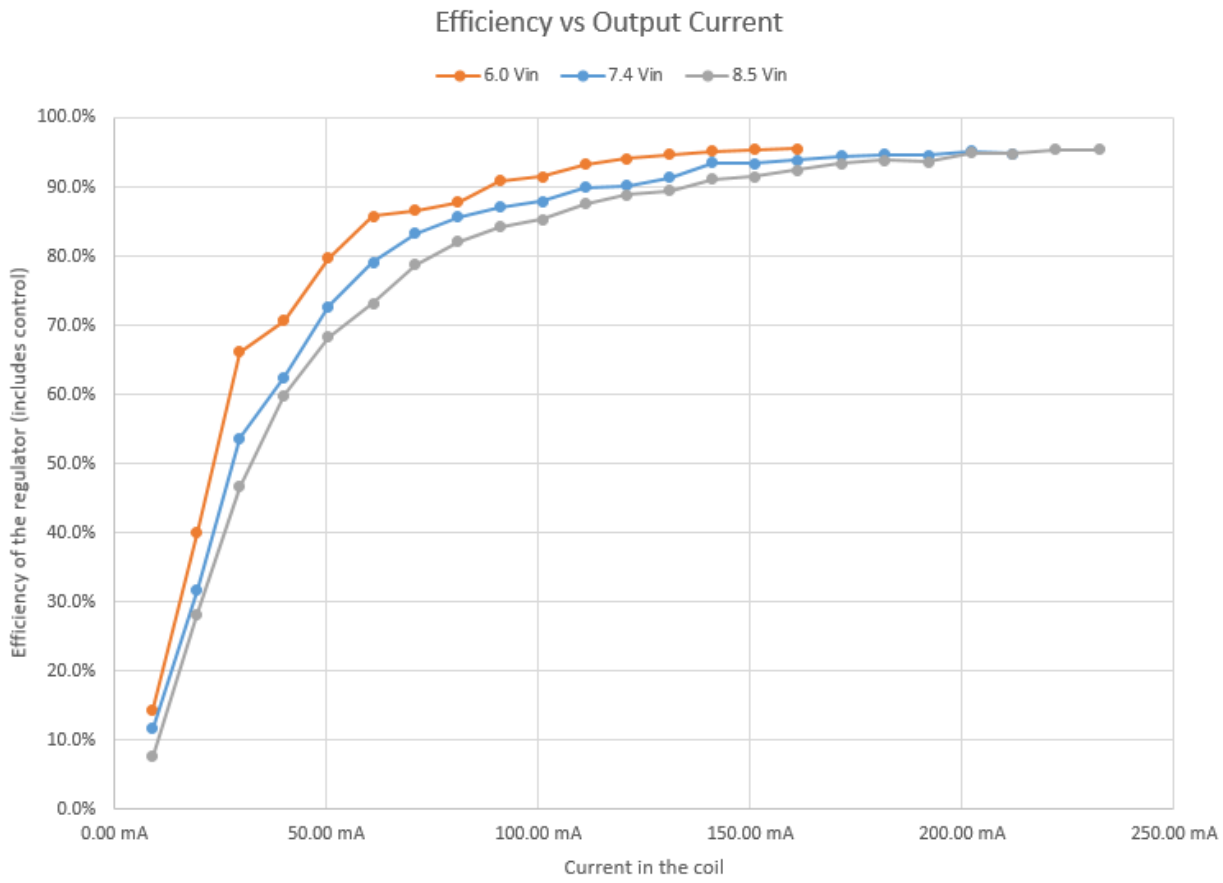

Figure 11: Measured efficiency verses output current of the final design.

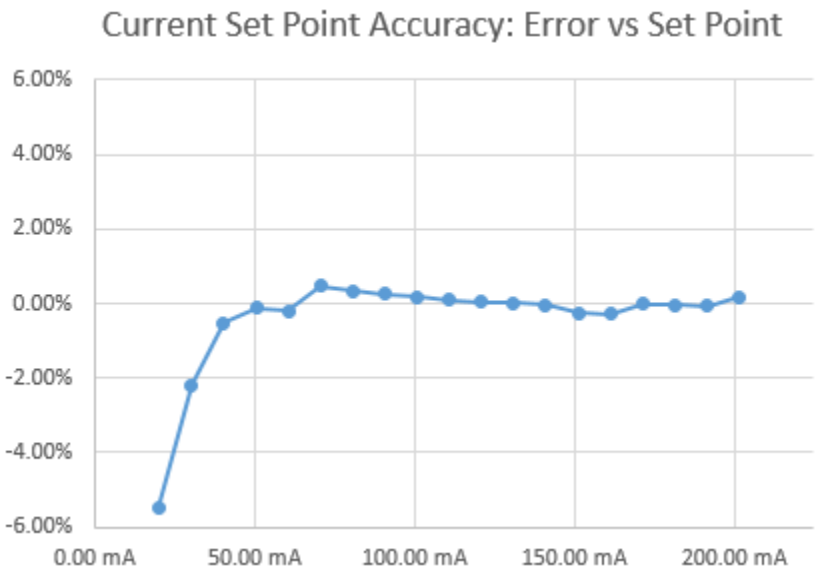

Figure 12: Current set point accuracy.

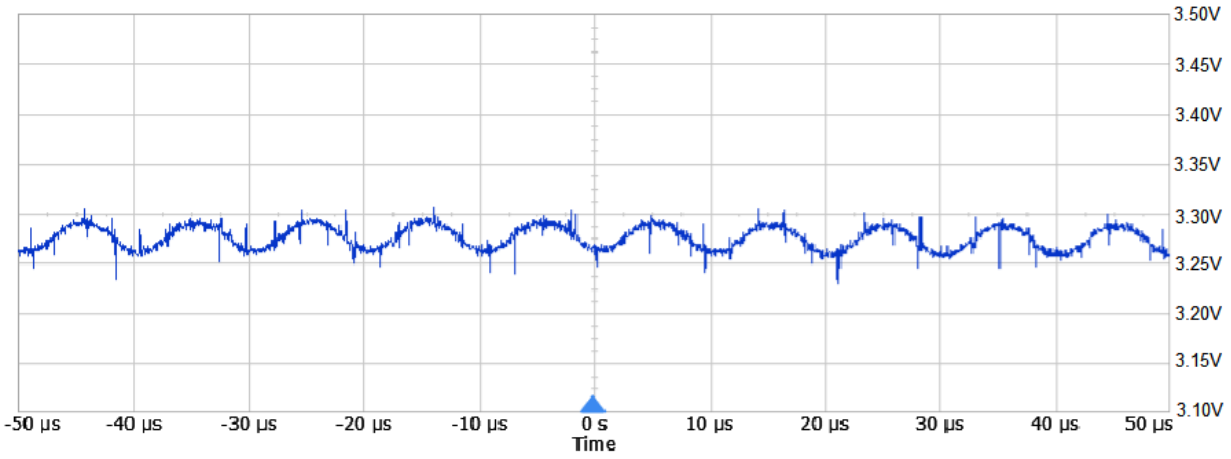

Figure 13: Output voltage ripple at 50% duty cycle.

Figure 13 shows the regulator's output voltage ripple at around 50% duty cycle. For a buck converter, 50% duty cycle is the point of maximum ripple. As seen in the figure, the peak-to-peak 100 kHz switching frequency noise is less than 50 mV peak to peak, which is even better than the original goal. Figure 14 shows the current regulator's output voltage during a sudden step from 50 mA output to 200 mA output. As seen in the figure, the transition occurs without ringing, and the output settles within 3 ms.

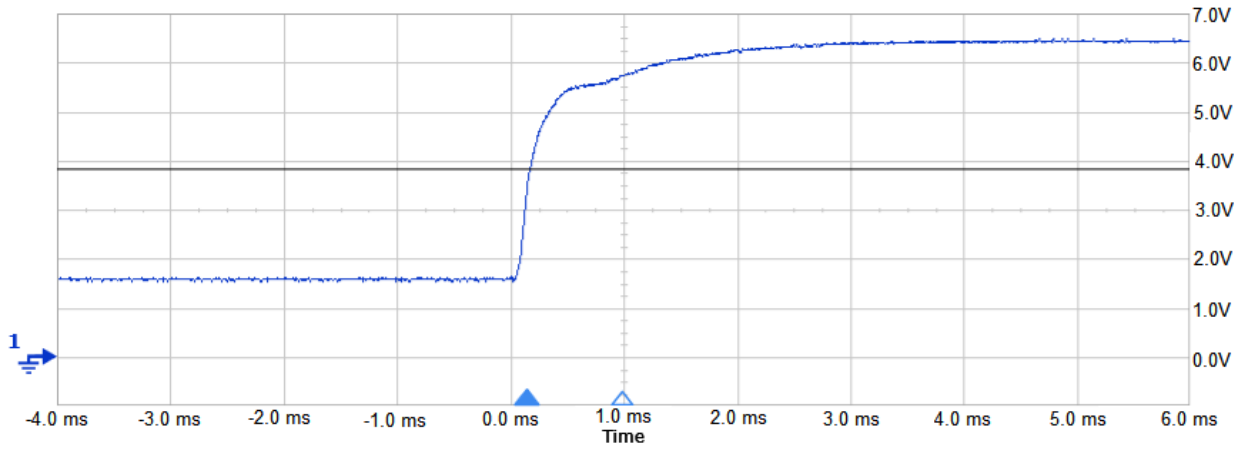

Figure 14: Step response measured on an oscilloscope.

Table 3: Quiescent power draw of torque coil components. lists the integrated circuit components of the torque coil, excluding only the unrelated gyroscope, along with their quiescent power consumptions. At nominal battery voltage, the total power consumption is only 22.2 mW per coil when not operating.

Table 3: Quiescent power draw of torque coil components.

Component	Part Number	Quiescent Current	Supply Voltage	Power Draw
Microcontroller	PIC18F24K22	2.5 mA	3.3 V	8.25 mW
RS-485 transceiver	LTC2850	0.37 mA	3.3 V	1.22 mW
PWM Oscillator	LTC6992-3	0.12 mA	3.3 V	0.40 mW
Op Amp (gain)	LT1783-6	0.23 mA	7.4 V nominal	1.70 mW
Op Amp (integrator)	LT1783-6	0.21 mA	3.3 V	0.69 mW
Gate Driver	TPS2836	0.25 mA	7.4 V nominal	1.85 mW
10-bit DAC	MCP4716	0.21 mA	3.3 V	0.69 mW
Precision 3V ref	MAX6029	5 µA	7.4 V nominal	0.04 mW
Low side H-bridge driver (x2)	UCC27517	0.20 mA (each)	7.4 V nominal	1.48 mW (each)
High side H-bridge driver (x2)	MIC5018	0.30 mA (each)	7.4 V nominal	2.22 mW (each)
			Total:	22.2 mW

6. Conclusion

In this project, I successfully designed, built, and tested a magnetic attitude control actuator for the University of Illinois' IlliniSat-2 CubeSat bus, which is going to space near the end of 2016. The current regulator I designed for this application met requirements for size and cost, along with numerous design goals for efficiency, low ripple, and fast response. This is the 7th revision of this design, because my last six revisions over the past two years were not fully functional. This project has been an incredible learning process for me as I tackled challenges in power electronics, controls, systems engineering, and practical PCB design, generally without any formal education in these areas. I am proud to conclude this project with a fully functional design, and to present this thesis describing my work.